Overview on the astrophysics of ultra-high energy cosmic rays

Jihyun Kim
Department of Physics
Ulsan National Institute of Science and Technology

2015-01-23
2015 Korea Numerical Astrophysics Group meeting @ KASI

Contents

Introduction to Ultra-High Energy Cosmic Rays

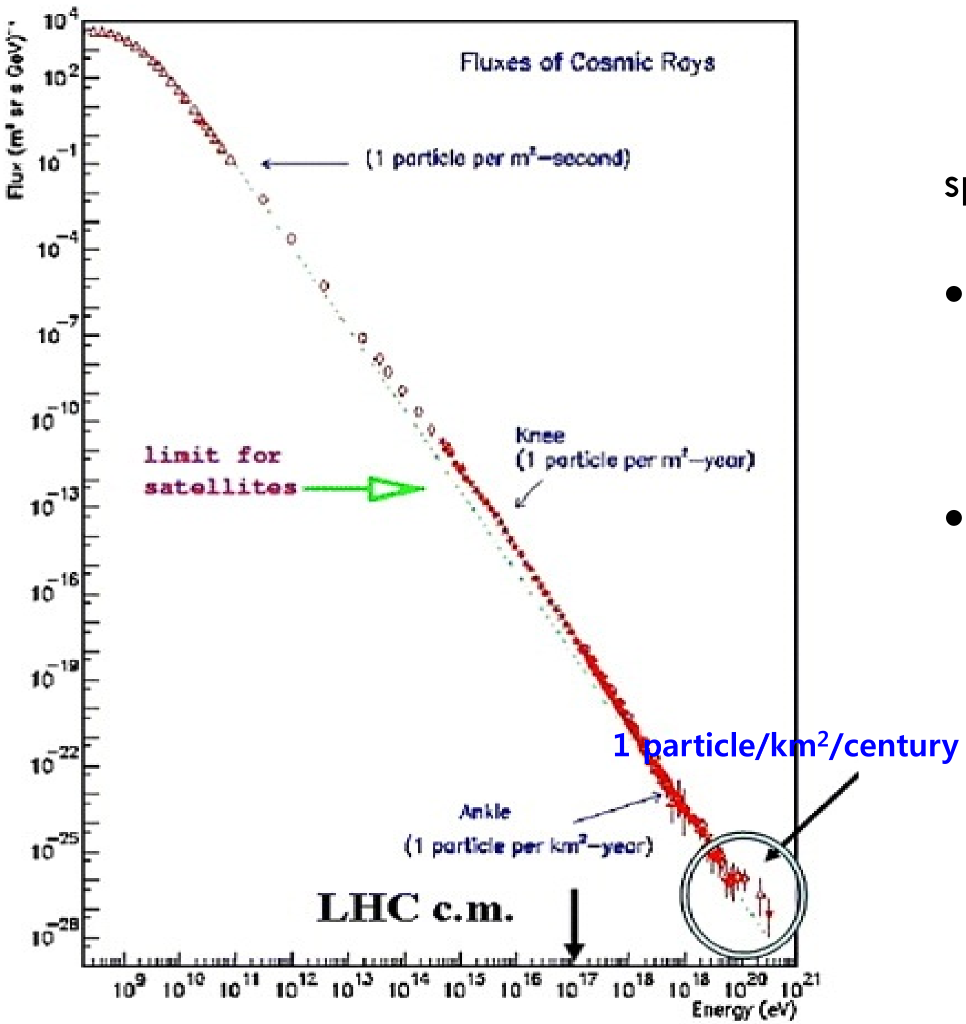

- Cosmic Rays

  : energetic particles originated from outer space that impinge on Earth's atmosphere.

- Ultra-High Energy Cosmic Rays

  : cosmic rays with energies above 10^{18} eV

- The mysteries of UHECRs
  - What are their components?

    → mass composition
  - Do they get through the GZK?

    → spectrum
  - Where do UHECRs come from?

    → arrival direction

Astrophysics of UHECRs

From production to observation

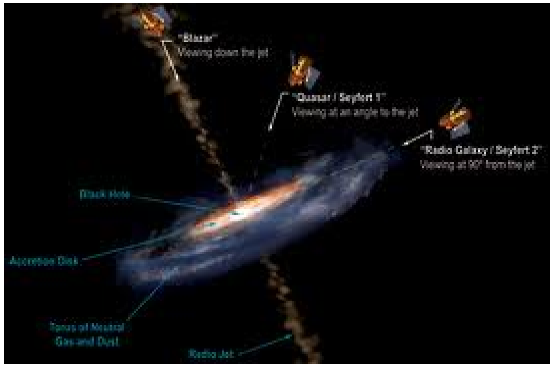

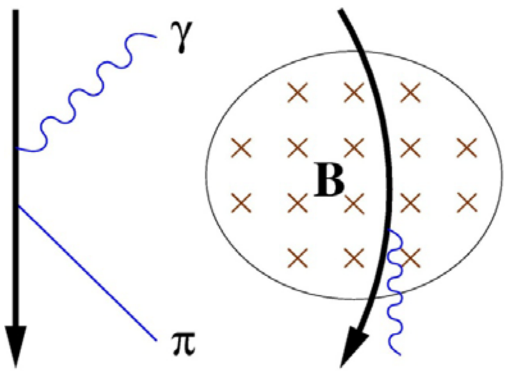

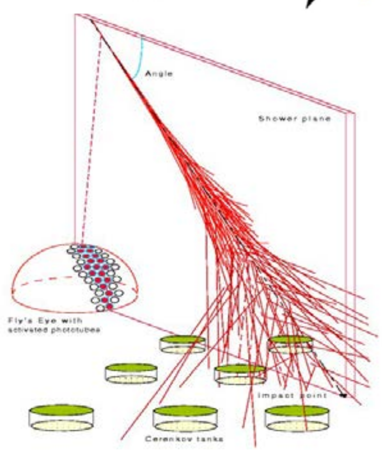

Production

- Acceleration of charged particles
- Decay of superheavy particles

Propagation

Cosmic background

Microwave, Radiowave, Magnetic fields

- Energy loss
- Secondary CR production
- Deflection

Observation

Atmosphere as caloriemeter/ scintillator

- Composition
- Energy
- Arrival Direction

Acceleration

- The maximum energy attainable by the diffusive acceleration in a certain astrophysical objects can be written by

$$E_{\max} = 4 \times 10^{20}\, Z \left(\frac{B}{100\mu\mathrm{G}}\right) \left(\frac{\beta_1}{0.3}\right) \left(\frac{D}{100\,\mathrm{kpc}}\right) \mathrm{eV}.$$

where Z is the atomic number

B is the magnetic field

β_1 is the Lorentz factor

D is the size of the astrophysical objects

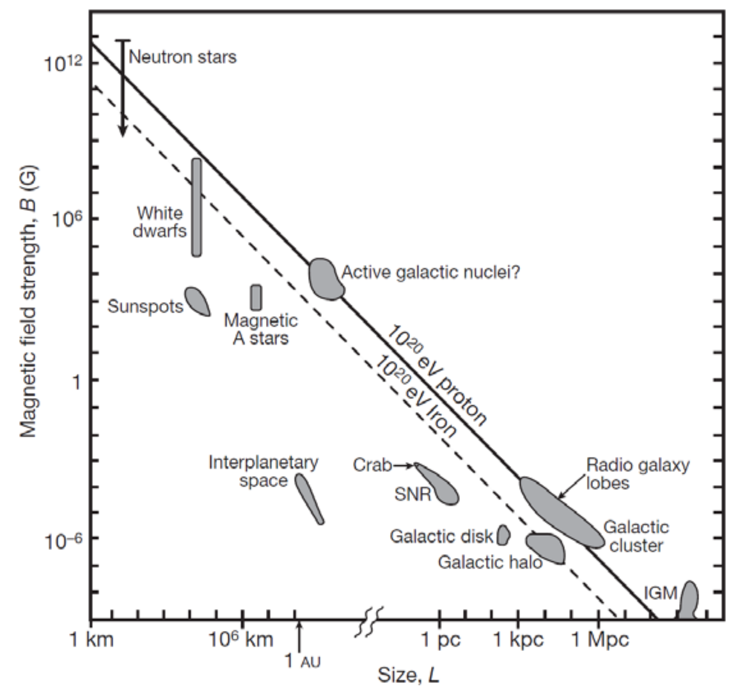

Bauleo and Martino (2009)

Propagation: energy loss

- When UHECRs propagate in the universe, they undergo attenuations. If we assume proton as a primary particle, we need to consider the energy losses by

$$\lambda^{-1} \equiv -\frac{1}{E}\frac{dE}{dx} = \lambda_z^{-1} + \lambda_{ee}^{-1} + \lambda_{\gamma\pi}^{-1}$$

  - redshift
  - pair production
  - photo-pion production (with CMB photon)

$$p + \gamma_{CMB} \rightarrow \pi + N$$

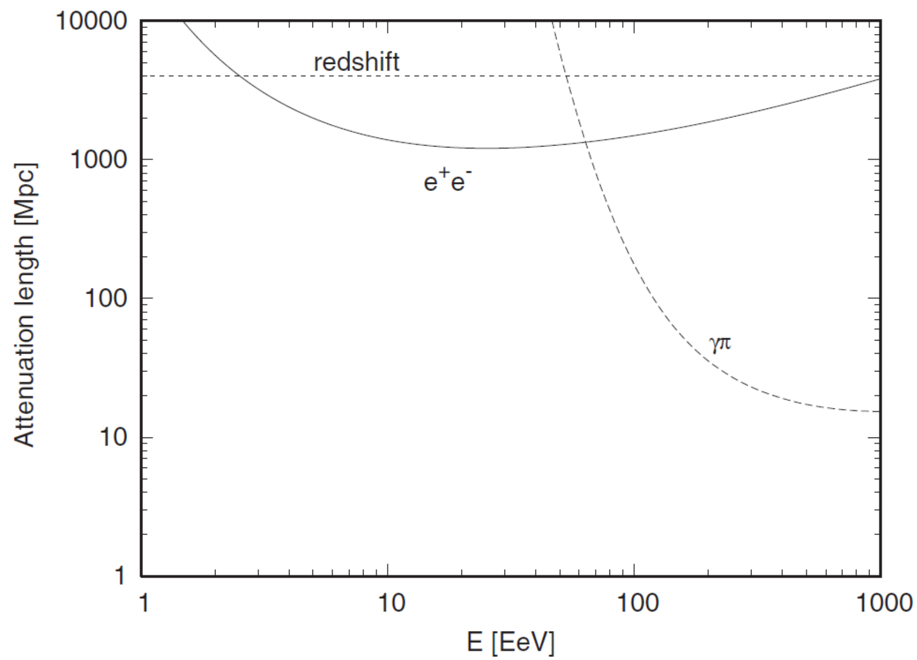

Harari et al. (2006)

Propagation: deflection

- Because UHECRs are charged particles, they can be deflected by galactic magnetic fields and extragalactic magnetic fields. The typical deflection using random patches of magnetic field is given by

$$\delta\theta = 0.8^\circ Z \left(\frac{E}{10^{20}\,\mathrm{eV}}\right)^{-1} \left(\frac{d\,l_c}{10\,\mathrm{Mpc}^2}\right)^{1/2} \left(\frac{B}{10^{-9}\,\mathrm{G}}\right)$$

where Z is the atomic number

E is the energy of UHECR

d is the distance

l_c is the average size of patches

B is the magnetic field

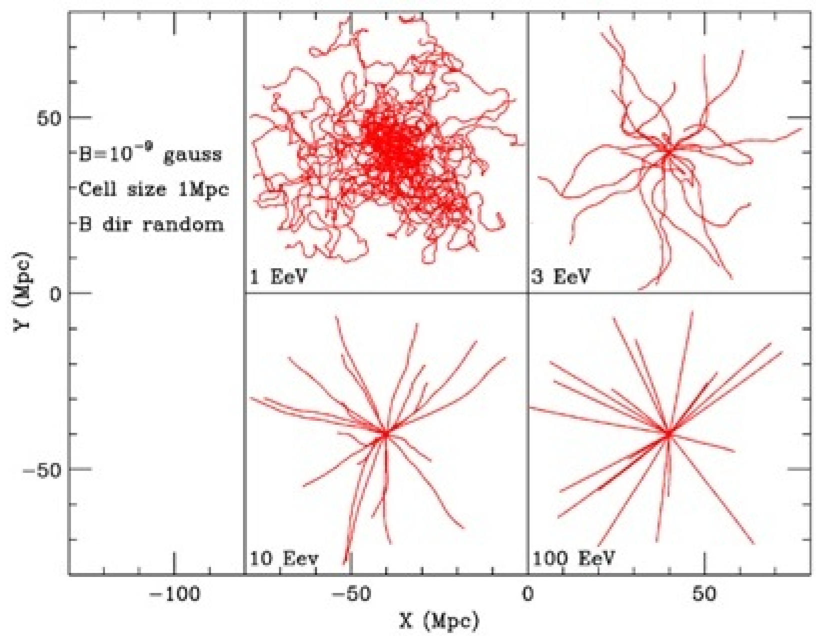

Extensive Air Showers

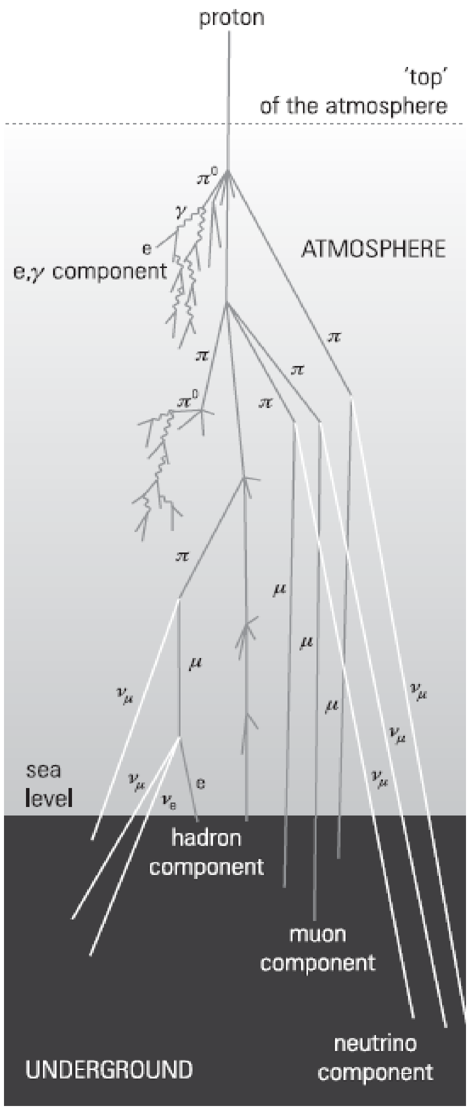

Extensive air showers (EAS):

- hadronic components
- muonic components
- electromagnetic components

Fluorescence detectors (FD):

observe fluorescence light generated in the atmosphere by charged electromagnetic particles

→ longitudinal distribution

→ estimate the mass composition of the primary particle

Surface detectors (SD):

detect the secondary particles of EAS survived at ground level

→ lateral distribution

→ estimate the energy of the primary particle

Recent Experiments

Recent Experiments

- Akeno Giant Air Shower Array (AGASA)
- High Resolution Fly's Eye (HiRes)
- Pierre Auger Observatory (PAO)
- Telescope Array (TA)

	AGASA	HiRes	PAO	TA
operation	1990-2004	1997-2006	2004-present	2008-present
detectors	111 SDs with 1 km spacing	2 FD stations with 12 km spacing	1600 SDs with 1.5 km spacing + 4 FD stations	507 SDs with 1.2 km spacing + 3 FD stations
spectrum	No GZK suppression	GZK suppression	GZK suppression	GZK suppression
composition		proton	proton + iron	proton
arrival direction	Isotropic Small-scale anisotropy	No significant correlation with nearby AGN	Correlation with nearby AGN ~ 0.38	No significant correlation with nearby AGN

Pierre Auger Observatory

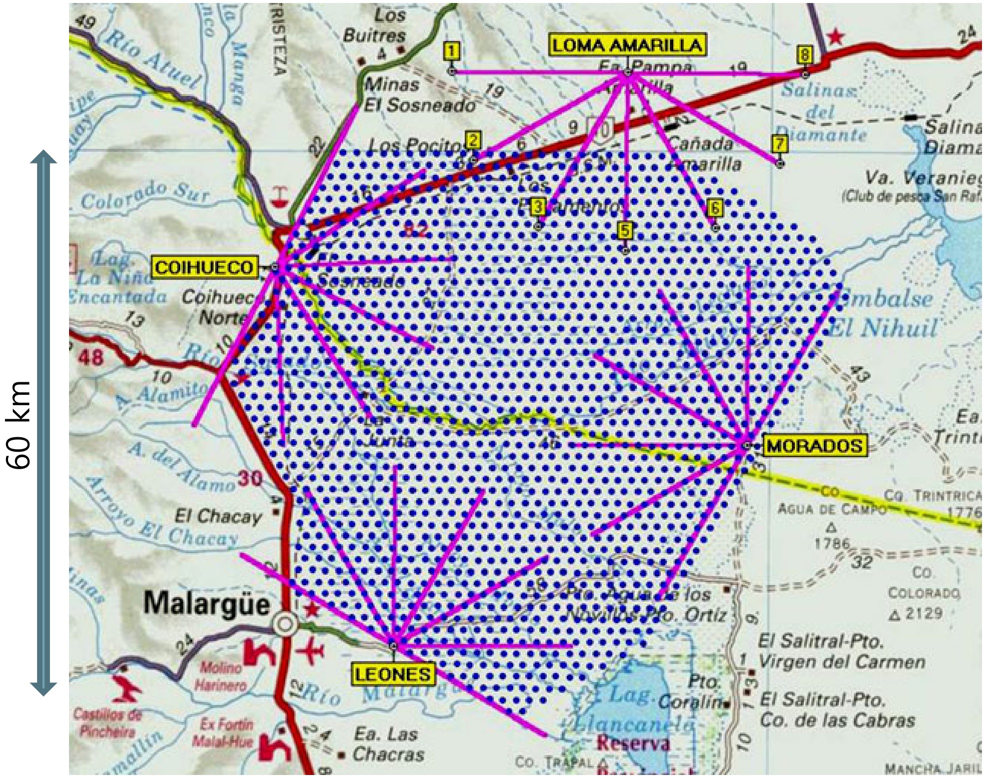

- Location : Mendoza, Argentina
- SD : 1600 water Cherenkov detector,
  1.5 km spacing, 3000 km^2
- FD : 24 telescopes in 4 stations

Surface Detector – Water Cherenkov

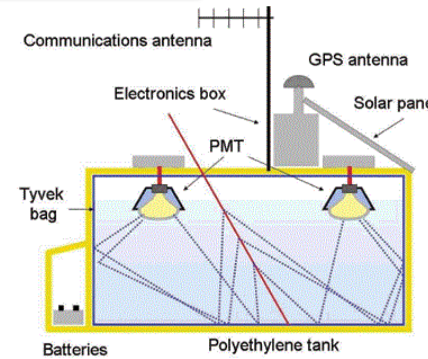

Fluorescence Detector – PMT

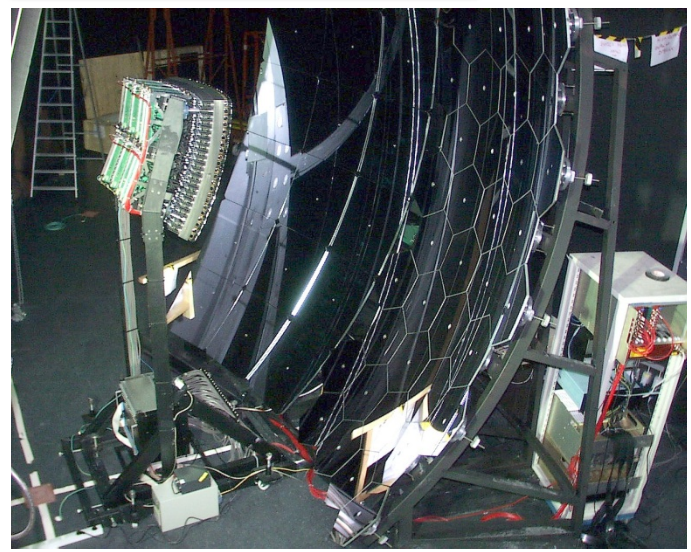

Telescope Array experiment

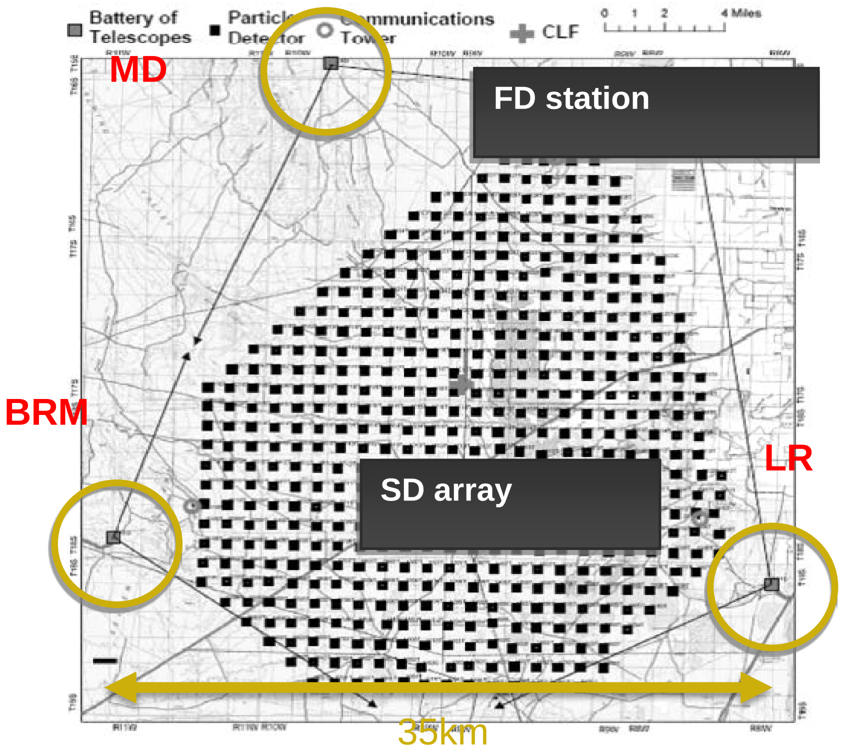

Surface Detector – Plastic Scintillation

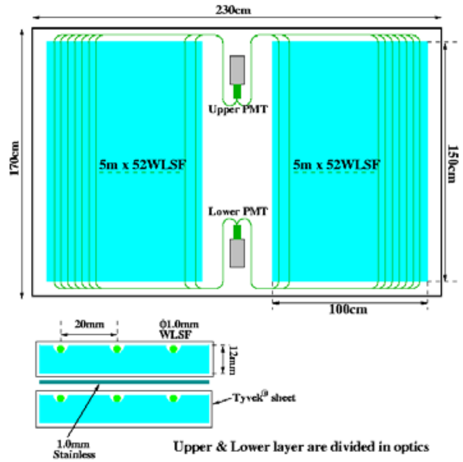

Fluorescence Detector – PMT

- Location : Utah, USA
- SD : 507 plastic scintillation detector,
  1.2 km spacing, 678 km^2
- FD : 18 telescopes in 3 stations

Spectrums

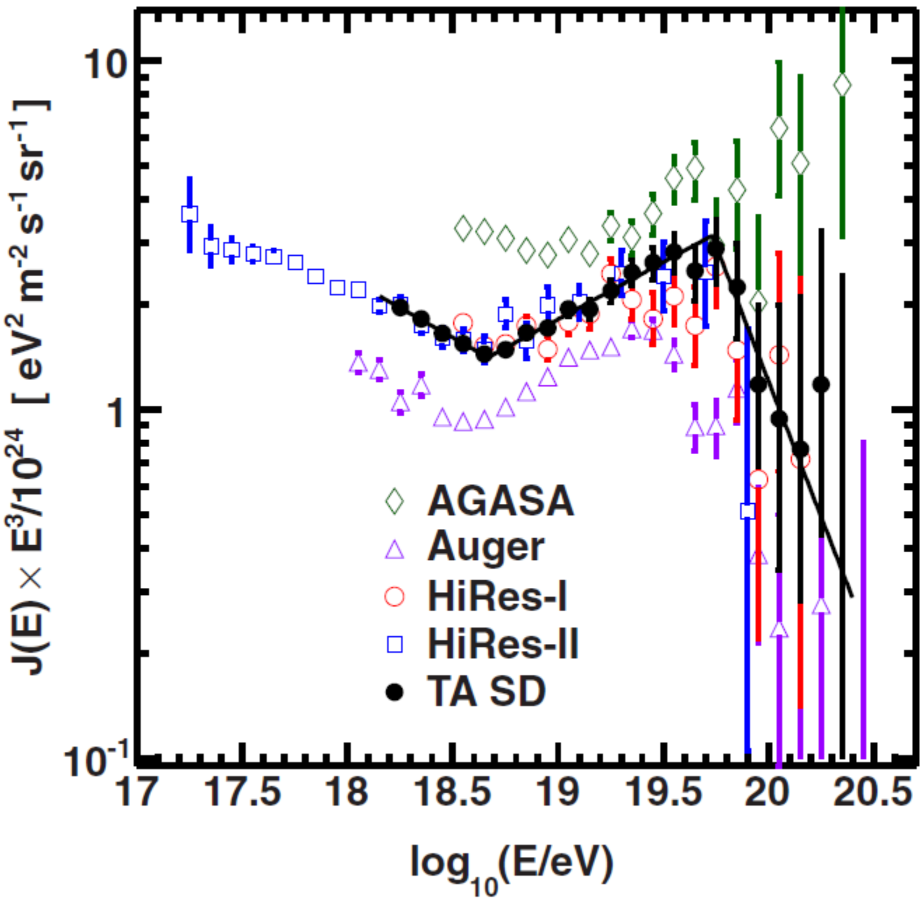

Abu-Zayyad et al. (2013)

Compositions

HiRes, TA : proton
PAO : transition from proton
to heavy nuclei

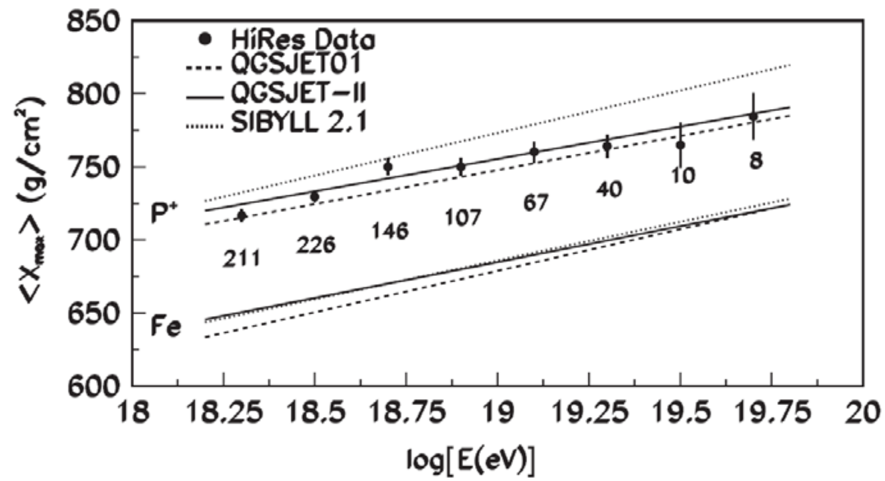

HiRes (Abbasi et al. 2010)

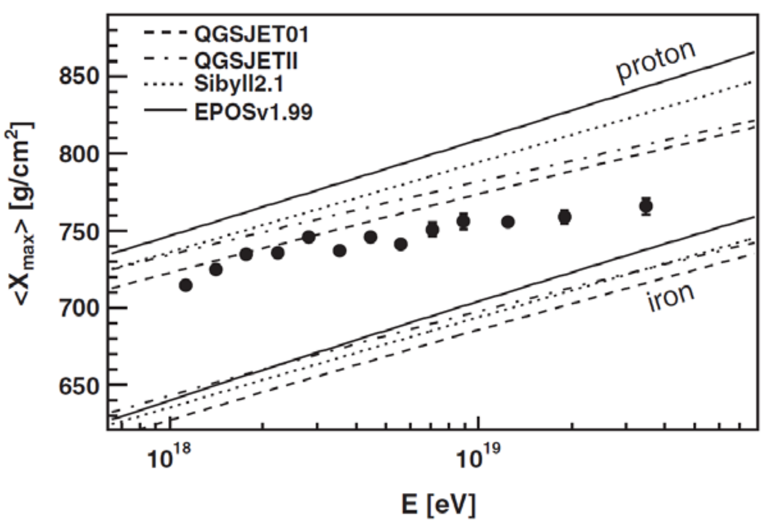

PAO (Abraham et al. 2010)

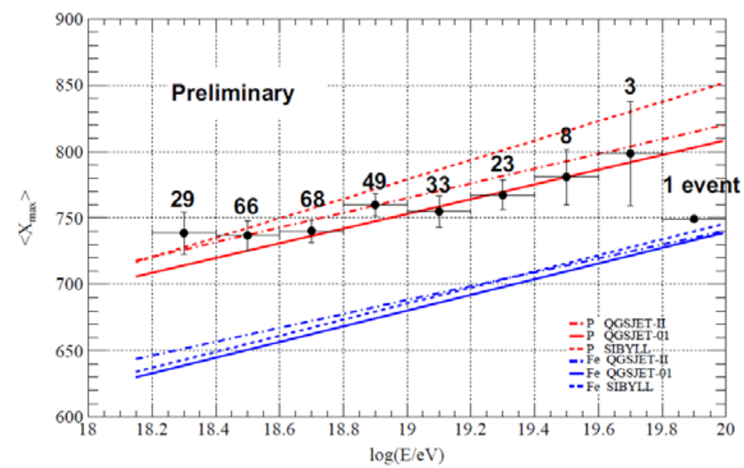

TA (Tameda et al. 2011)

Arrival direction distributions

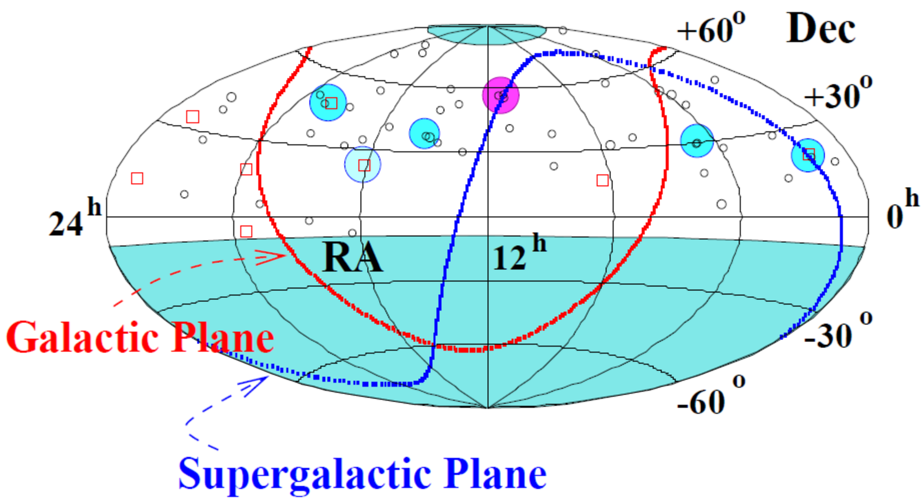

AGASA (Hayashida et al. 2000)

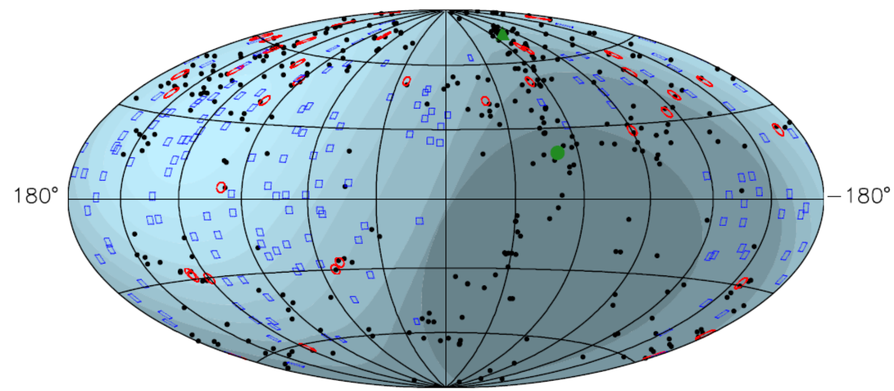

HiRes (Abbasi et al. 2008)

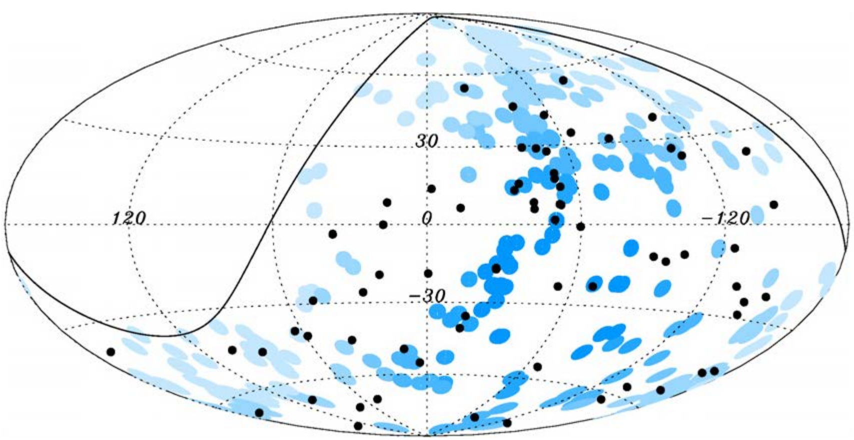

PAO (Abreu et al. 2010)

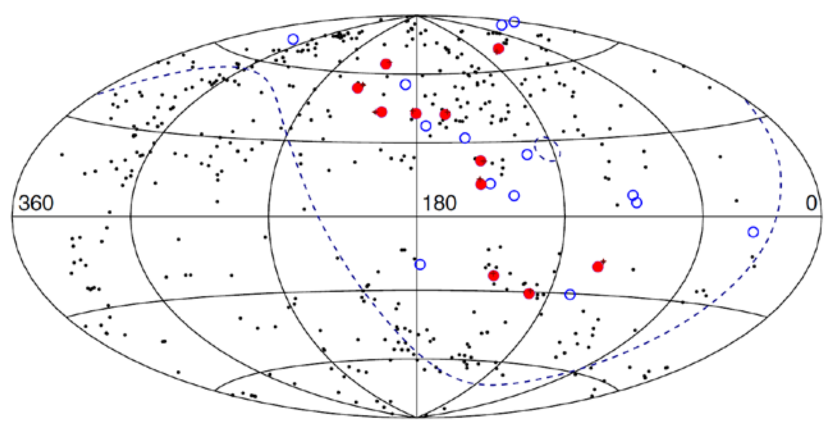

TA (Abu-Zayyad et al. 2012)

Methodologies to figure out the origin of UHECR using Arrival Direction Distributions

Strategy

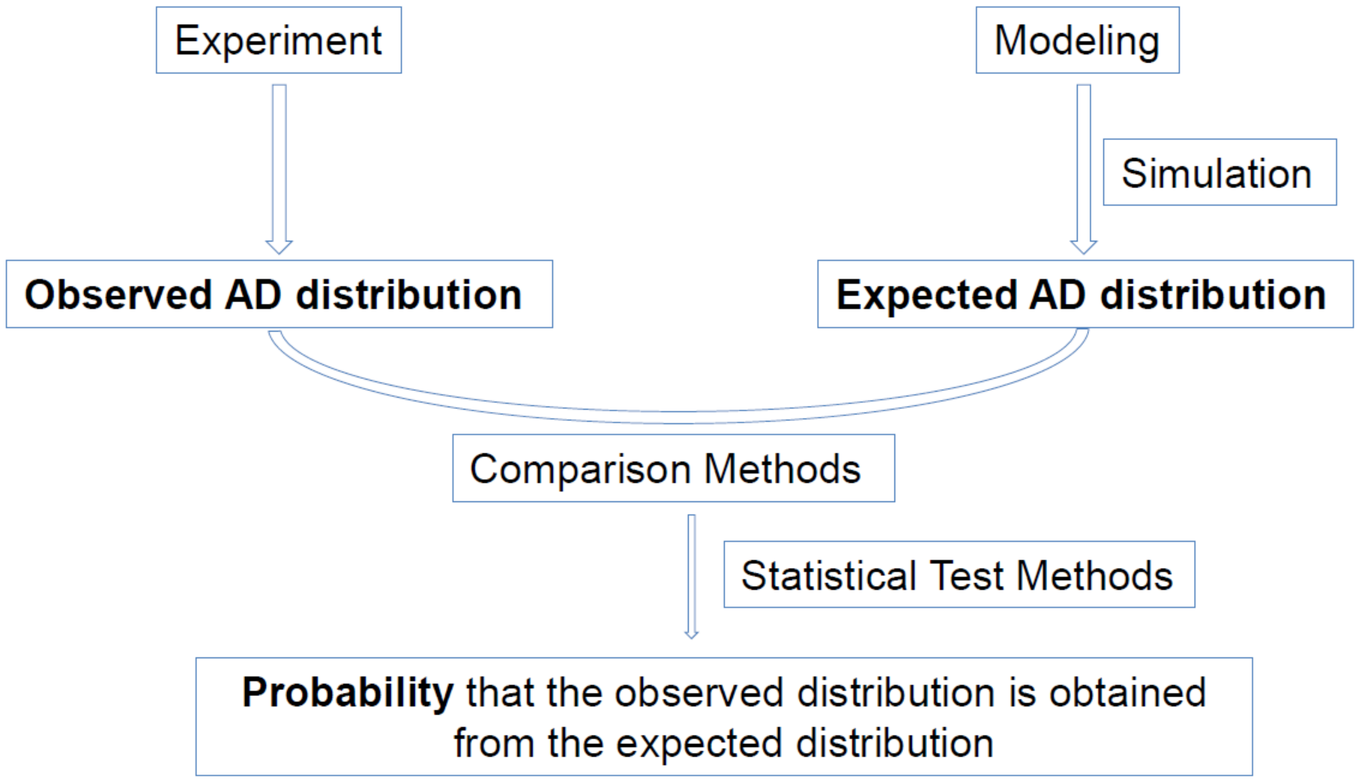
Experiment
Modeling
Simulation
Observed AD distribution
Expected AD distribution
Comparison Methods
Statistical Test Methods
Probability that the observed distribution is obtained from the expected distribution

Source Models

- The expected flux at a given arrival direction can be written as the sum of two contributions,

$$\begin{aligned} F(\hat{\mathbf{r}}) &= F_{\rm src}(\hat{\mathbf{r}}) + F_{\rm iso}, \\ &= f_s \overline{F} \frac{\exp\left[-\left(\theta_j(\hat{\mathbf{r}})/\theta_s\right)^2\right]}{N(\theta_s)} + (1 - f_s)\overline{F} \end{aligned}$$

where

$$f_s = \frac{\overline{F}_{\rm src}}{\overline{F}_{\rm src} + F_{\rm iso}}$$: the source fraction

$$\theta_j(\hat{\mathbf{r}}) = \arccos(\hat{\mathbf{r}} \cdot \hat{\mathbf{r}}'_j)$$: the smearing angle

$$\overline{F} = \overline{F}_{\rm src} + F_{\rm iso}$$

$$N(\theta_{sj}) = (1/4\pi) \int d\Omega \exp[-(\theta_j(\hat{\mathbf{r}})/\theta_{sj})^2]$$

Geometrical exposure function

- If there is UHECR detector located at latitude λ and its efficiency limit the detectable zenith angle of UHECR to θ_m. The arrival direction of a incident UHECR is (α, δ) and its zenith angle is θ,

$$h(\delta) = \frac{1}{\pi}\left[\sin\alpha_m \cos\lambda\cos\delta + \alpha_m \sin\lambda\sin\delta\right]$$

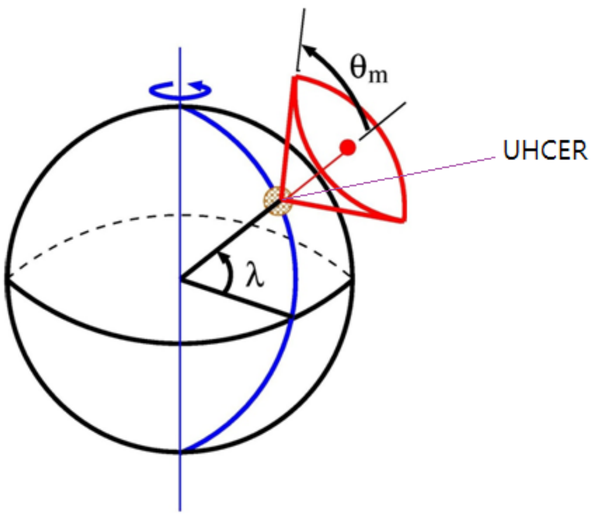

where

$$\alpha_m = \begin{cases} 0, & \text{for } \xi > 1, \\ \pi, & \text{for } \xi < -1, \\ \arccos\xi, & \text{otherwise} \end{cases} \quad \text{with } \xi = \frac{\cos\theta_m - \sin\lambda\sin\delta}{\cos\lambda\cos\delta}$$

Reduction Methods

- Auto-Angular Distance Distribution (AADD)

  : the distribution of the angular distances of all pairs of UHECR arrival directions themselves

$$\text{AADD: } \{\cos\theta_{ij} \equiv \hat{\mathbf{r}}_i \cdot \hat{\mathbf{r}}_j \mid i, j = 1, \ldots, N\}$$

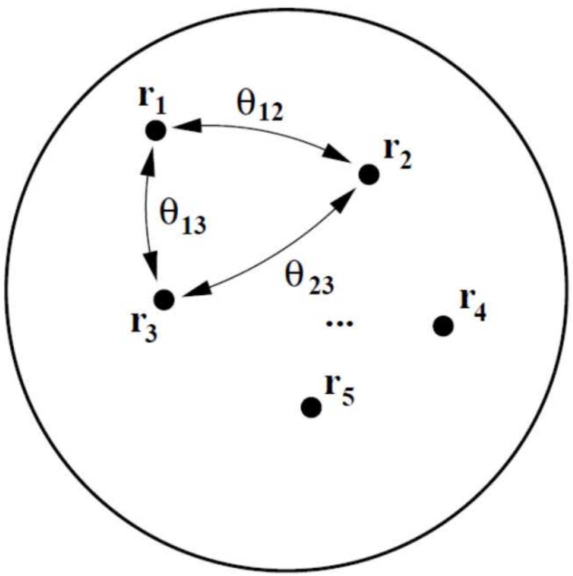

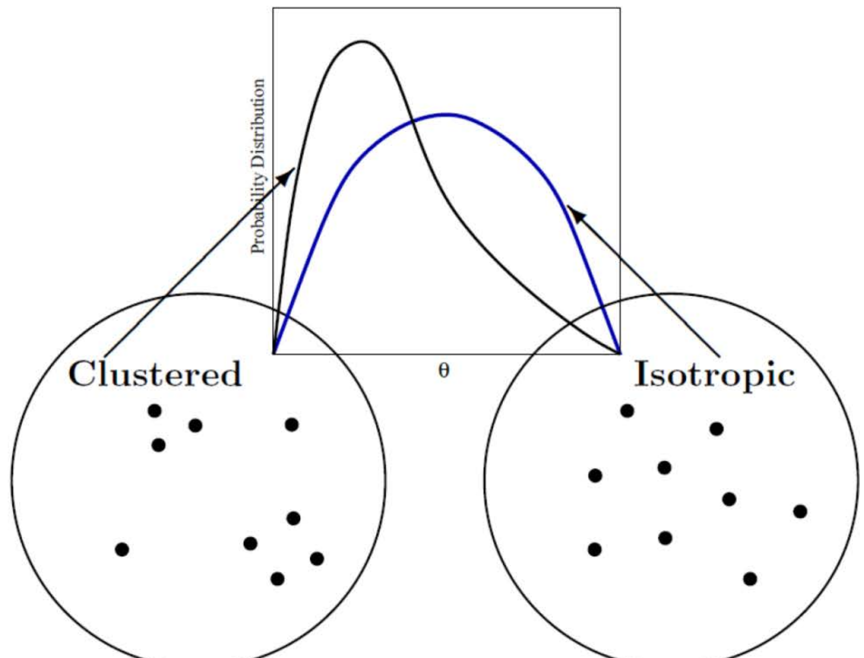

Reduction Methods

- Correlational Angular Distance Distribution (CADD)

  : the distribution of the angular distances of all pairs UHECR arrival directions and the point source directions

$$\text{CADD:}\ \left\{\cos\theta_{ij'} \equiv \hat{\mathbf{r}}_i \cdot \hat{\mathbf{r}}'_j \mid i = 1,\ldots,N;\ j = 1,\ldots,M\right\}$$

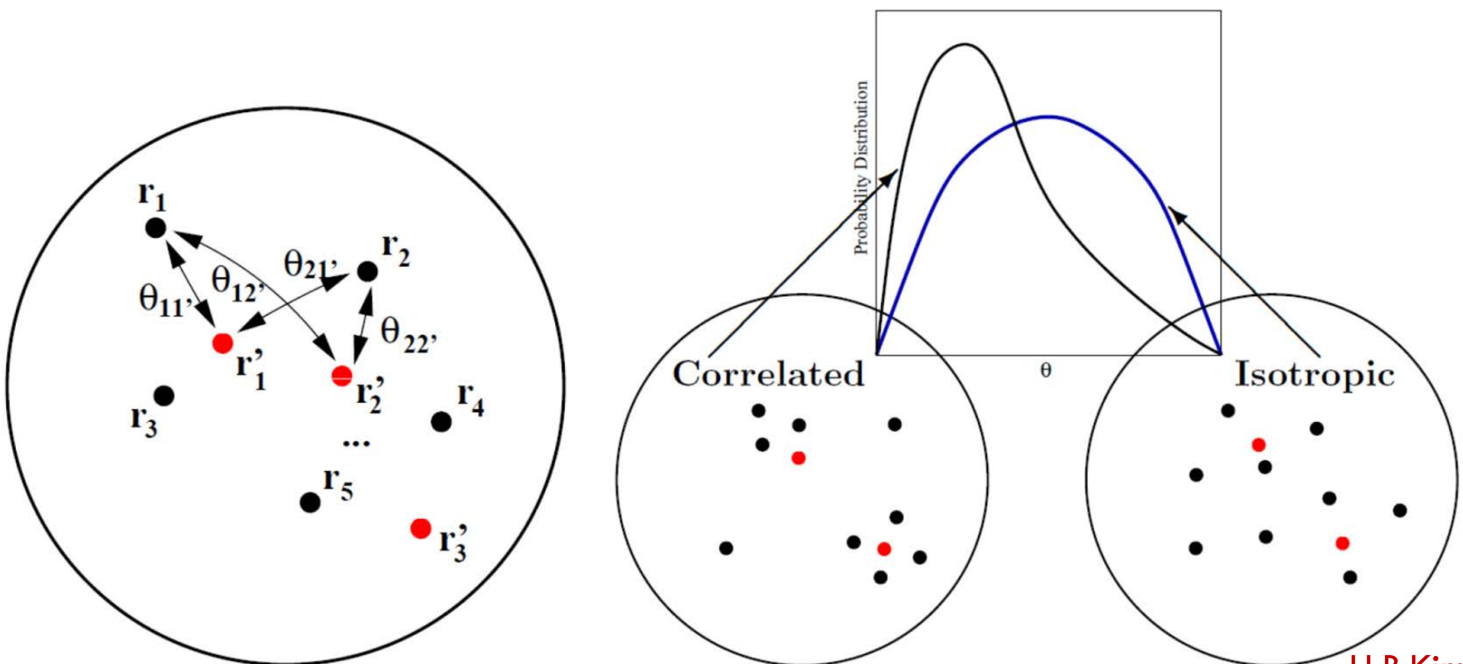

H.B.Kim & JK (2011)
H.B.Kim & JK (2013)

Reduction Methods

- Nearest-neighbor Angular Distance Distribution (NADD)

  : the distribution of the angular distances between the arrival directions of UHECR and those of nearest-neighboring sources.

$$\text{NADD:}\ \left\{ \phi_i \equiv \min_{j'}(\cos\theta_{ij'}) \mid i = 1, \ldots, N;\ j = 1, \ldots, M \right\}$$

Statistical Test Methods

- Kolmogorov-Smirnov test

$$D_{\mathrm{KS}} = \max_x |S_O(x) - S_E(x)|$$

$$P_{\mathrm{KS}}(D_{\mathrm{KS}}|N_e) = Q_{\mathrm{KS}}([\sqrt{N_e} + 0.12 + 0.11/\sqrt{N_e}]D_{\mathrm{KS}})$$

where $Q_{\mathrm{KS}}(\lambda) \; = \; 2\sum_{j=1}^{\infty}(-1)^{j-1}e^{-2j^2\lambda^2}$

$$N_e = N_O\, N_E/(N_O + N_E)$$

- Anderson-Darling test

$$D_{\mathrm{AD}} = \max_x \frac{|S_O(x) - S_E(x)|}{\sqrt{S_O(x)(1 - S_E(x))}}$$

Statistical Test Methods

- Kuiper test

$$D_{\mathrm{KP}} = \max_x [S_O(x) - S_E(x)] + \max_x [S_E(x) - S_O(x)]$$

$$P_{\mathrm{KP}}(D_{\mathrm{KP}}|N_e) = Q_{\mathrm{KP}}([\sqrt{N_e} + 0.155 + 0.24/\sqrt{N_e}]D_{\mathrm{KP}})$$

where $Q_{\mathrm{KP}}(\lambda) = 2\sum_{j=1}^{\infty}(4j^2\lambda^2 - 1)e^{-2j^2\lambda^2}$

- How to get probability for AADD/CADD

We simulate the same number of UHECR as the observed data from the source model, reference set. Using this, we calculate the KS/KP statistic and repeat this procedure 10^4 times. Then we can infer the significance of D_{obs} from 10^4 D_{ref} pool. Therefore, our probability estimate is reliable up to roughly 10^{-4}.

Description of the observation data

Data Description: PAO and TA

	PAO	TA
operation	2004-01-01 to 2009-12-31 (full six-year)	2008-05-11 to 2011-09-15 (about 40-months)
energy threshold	5.5×10^{19} eV	5.7×10^{19} eV
latitude and zenith angle cut	35.1°S, 60° (24.9°N-90°S)	39°N, 45° (84.3°N-5.7°S)
# of events	69 events	25 events

The energy threshold of the observational data is,
$E_c = 5.5\times10^{19}$ eV.

Search for the Correlation with AGN in the PAO/TA

The Veron-Cettiy and Veron Catalog

d_c = 100 Mpc

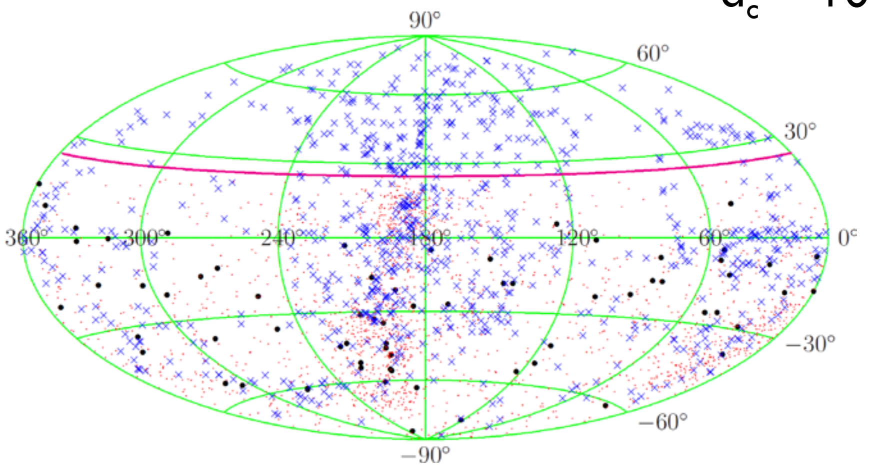

69 UHECR / 600 AGN

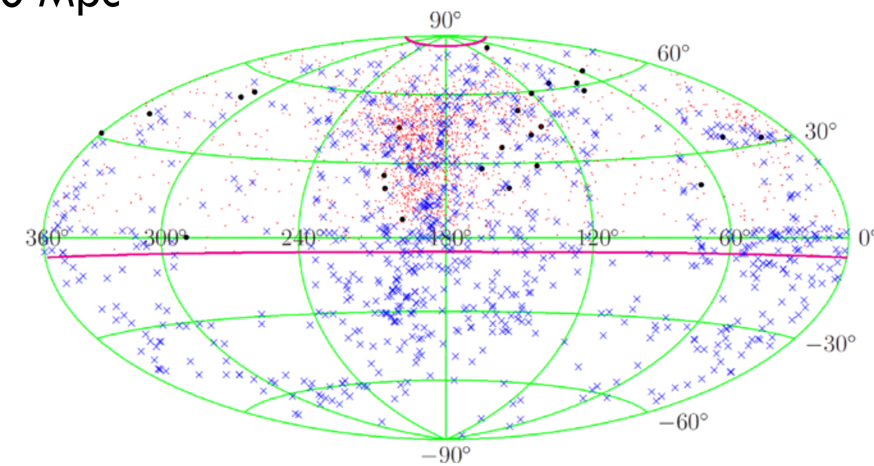

42 UHECR / 599 AGN

Hammer projection of PAO-VCV/TA-VCV skymap in equatorial coord.

black bullets: observed UHECRs AD

blue asterisks: 862 AGN from the VCV catalog

red dots: 2000 mock UHECRs AD with f_s=0.7 & w_s=10

magenta line: Field of view for each site

The VCV catalog: results

- CADD/NADD parameter estimate

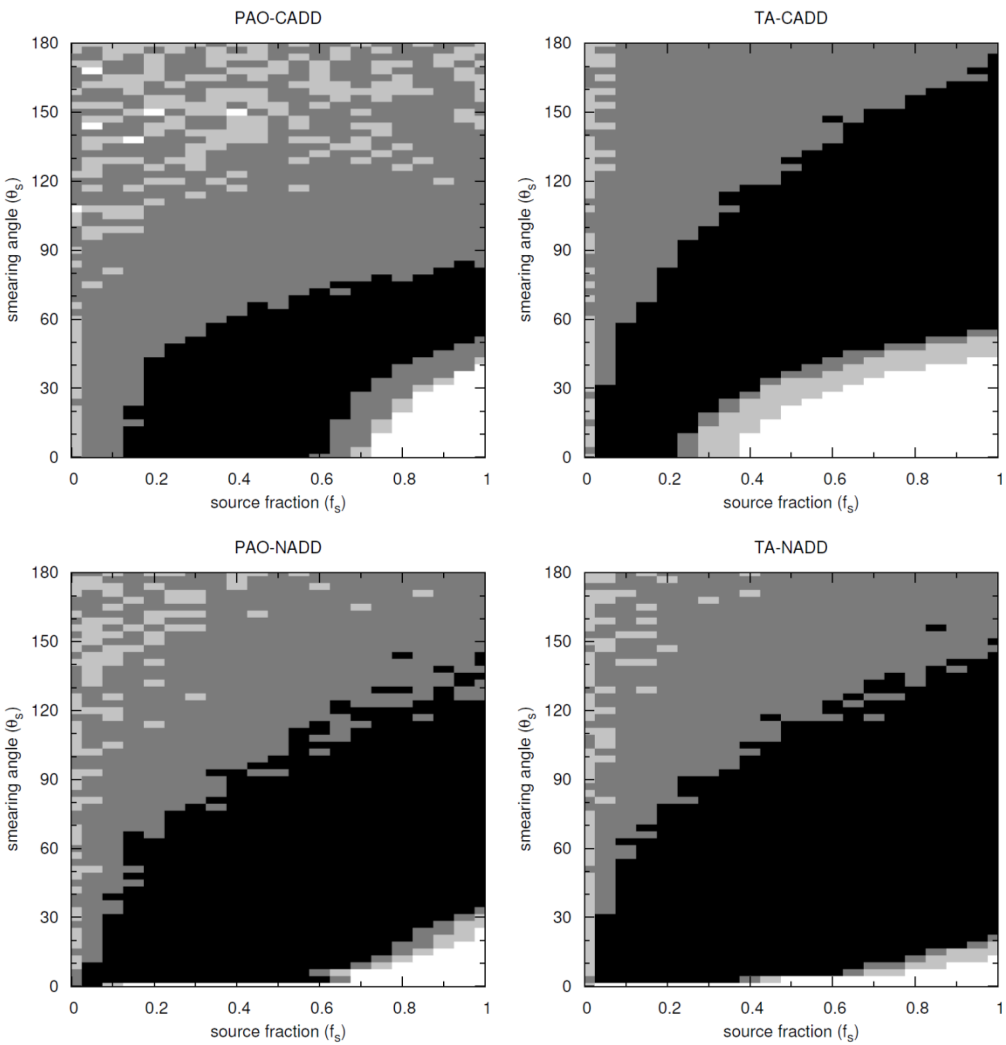

excluded source models
3σ confidence level

	PAO	TA
CADD	$f_s \geq 0.7$ $\theta_s \leq 40°$	$f_s \geq 0.4$ $\theta_s \leq 40°$
NADD	$f_s \geq 0.7$ $\theta_s \leq 40°$	$f_s \geq 0.8$ $\theta_s \leq 15°$

→ AGN dominance models with relatively small smearing angles are rejected.

best values by
the parameter estimation

	PAO	TA
CADD	(0.40, 0°)	(0.90, 72°)
NADD	(0.25, 3°)	(1.00, 51°)

The VCV catalog: results

- CADD/NADD with w=3°

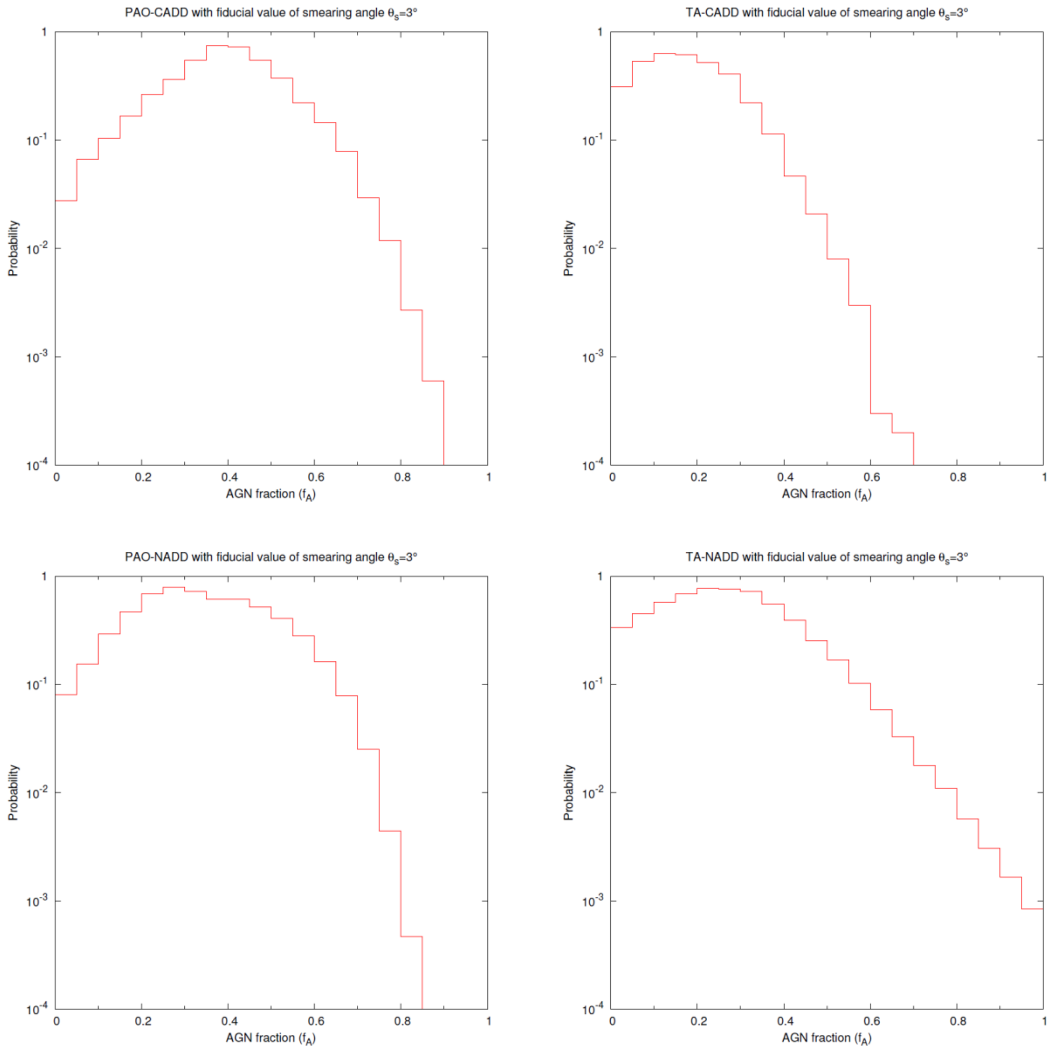

best value with w=3°

	PAO	TA
CADD	$f_s = 0.35$	$f_s = 0.10$
NADD	$f_s = 0.25$	$f_s = 0.20$

$f_s = 0.7$ (Koers and Tinyakov, 2009) assuming the uniform background outside the GZK radius

require more isotropic components!

The VCV catalog: results

- CADD/NADD with r=0.7

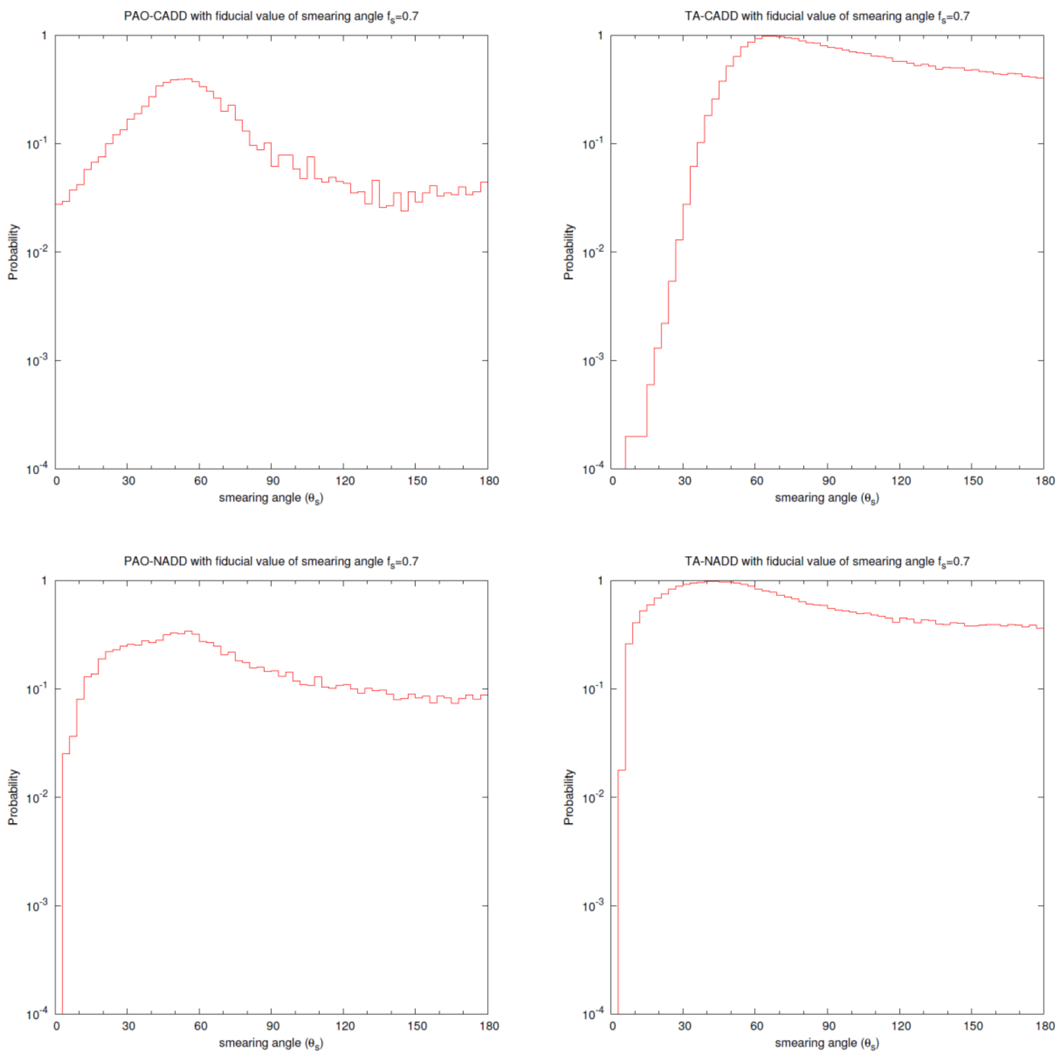

best value with f_x=0.7

	PAO	TA
CADD	$\theta_s = 54°$	$\theta_s = 66°$
NADD	$\theta_s = 54°$	$\theta_s = 39°$

conventional deflection angle by the magnetic field
- proton: ~ 3°
- iron: ~ 70°

require larger deflection angle!

The VCV catalog: discussion

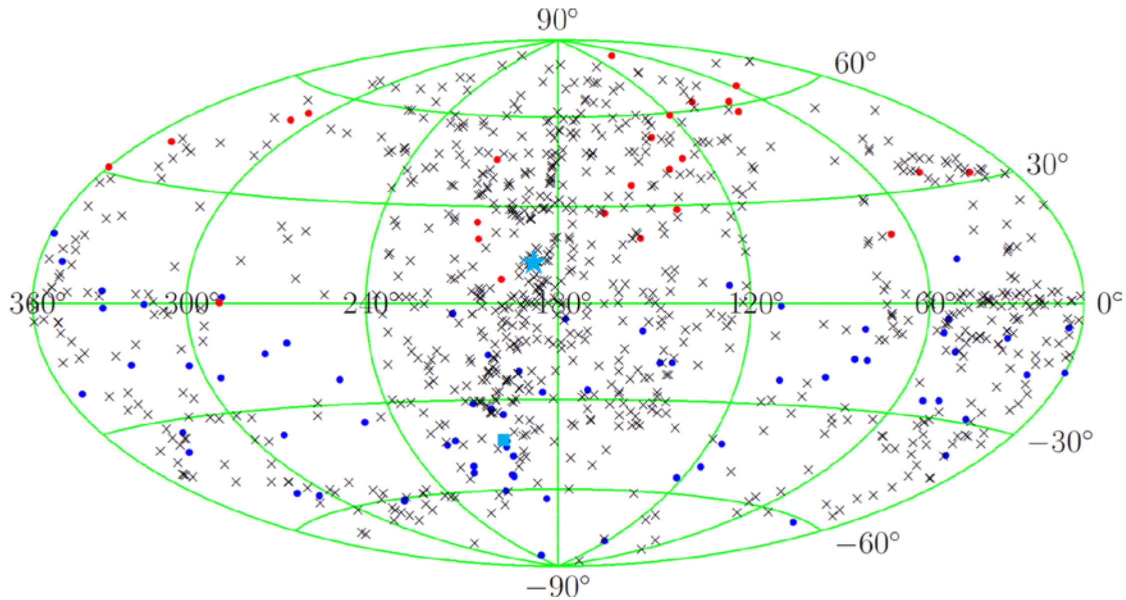

Hammer projection of PAO-TA-VCV skymap in equatorial coord.

blue bullets: 69 PAO UHECRs
red bullets: 25 TA UHECRs
cyan squares: Centaurus A
cyan star: M87

Conclusions

Conclusions

- The observed UHECR distributions require more isotropic components in the source model. If we assume AGN or a subset of AGN are the origin of UHECRs, we can extend this results for
  - estimating the magnitude of the intervening magnetic fields

    The strong magnetic field than the conventional one is needed.

    Ryu et al. (Ryu et al., 2010) suggest the average deflection angle of protons is about 15°.

  - identifying the primary particles

    The measurement of X_{max} from PAO (Abraham et al., 2010) show that the primary particles would be heavier ones with increasing their energies. Dermer et al. (Dermer & Razzaque, 2010) conclude that heavy nuclei are more likely to be accelerated to ultra-high energy in AGNs.

Most up-to-date observational data

Most up-to-date result of TA [ApJL 790, L21 (2014)]

- observation period: from 2008-05-11 to 2013-05-04
- zenith angle: $\theta \leq 55°$
- energy range: $E \geq 57$ EeV
- # of UHECR events = 72

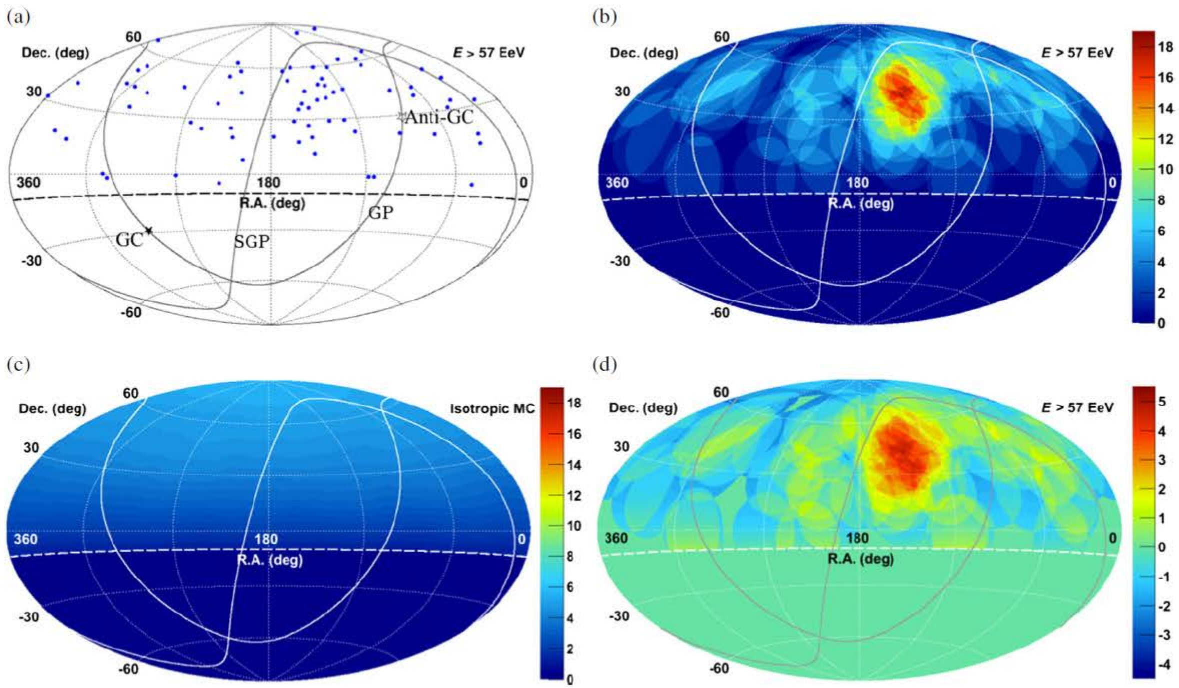

Figure 1. Aitoff projection of the UHECR maps in equatorial coordinates. The solid curves indicate the galactic plane (GP) and supergalactic plane (SGP). Our FoV is defined as the region above the dashed curve at decl. = −10°. (a) The points show the directions of the UHECRs $E > 57$ EeV observed by the TA SD array, and the closed and open stars indicate the Galactic center (GC) and the anti-Galactic center (Anti-GC), respectively; (b) color contours show the number of observed cosmic-ray events summed over a 20° radius circle; (c) number of background events from the geometrical exposure summed over a 20° radius circle (the same color scale as (b) is used for comparison); (d) significance map calculated from (b) and (c) using Equation (1).

Most up-to-date result of PAO [arXiv:1411.6111]

- observation period: from 2004-01-01 to 2014-03-31
- zenith angle: $\theta \leq 80°$
- energy range: $E \geq 52$ EeV
- # of UHECR events = 231

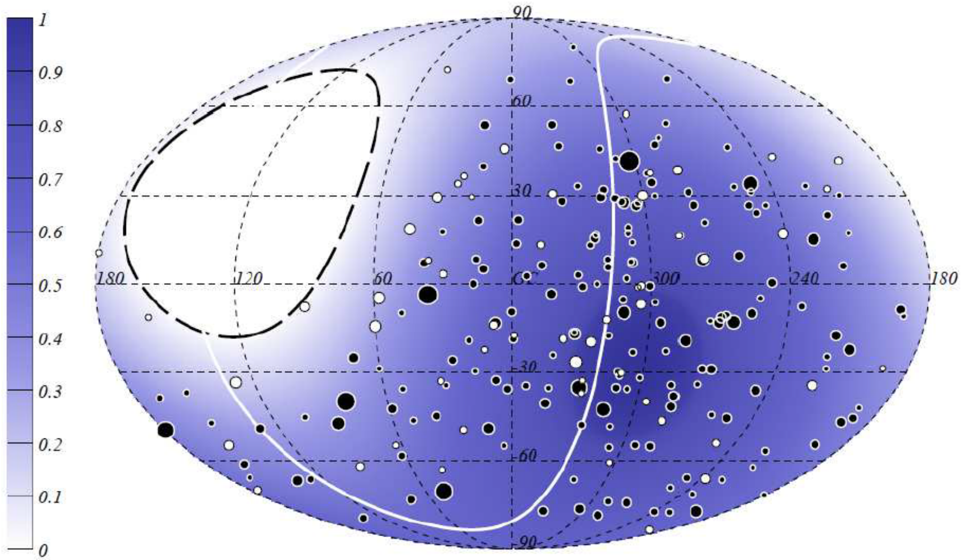

Fig. 11.— Map in Galactic coordinates of the arrival directions of the events with $E \geq$ 52 EeV. The black (white) circles correspond to *vertical* (*inclined*) events. The size of each circle scales with the energy of the event. The color scale is proportional to the relative exposure.

JEM-EUSO (planned)

- The Extreme Universe Space Observatory, on-board the Japanese Experiment Module (JEM-EUSO) of the International Space Station
- JEM-EUSO is currently designed to meet a launch date in 2017.

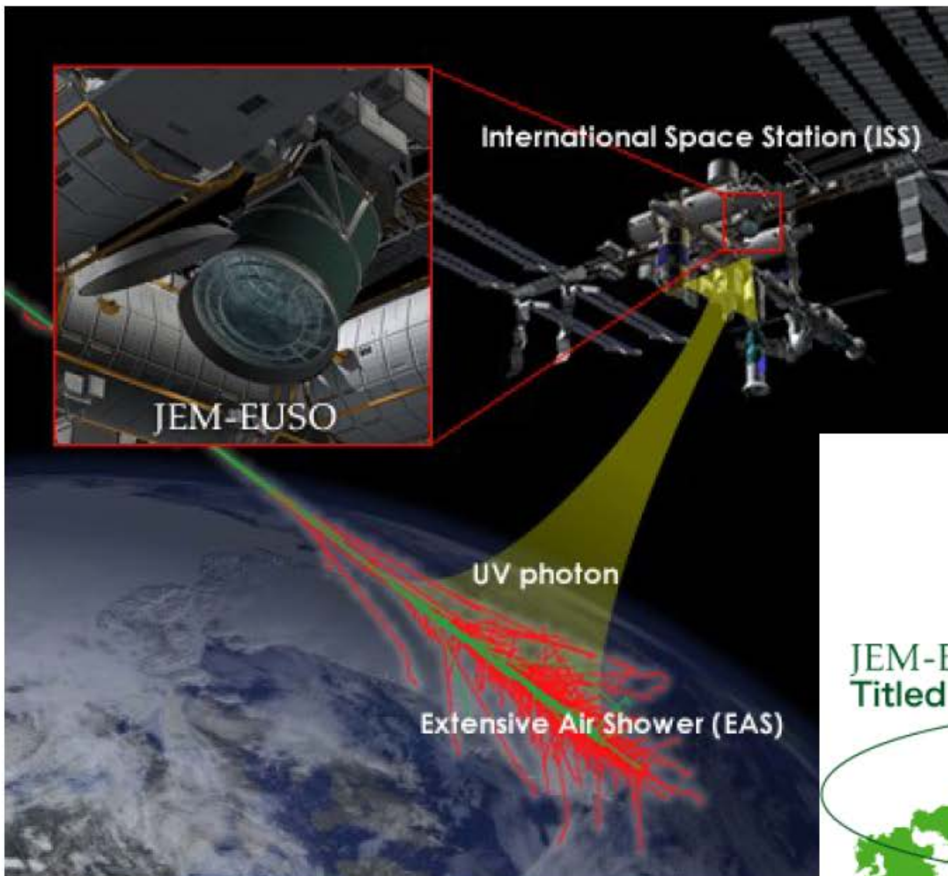

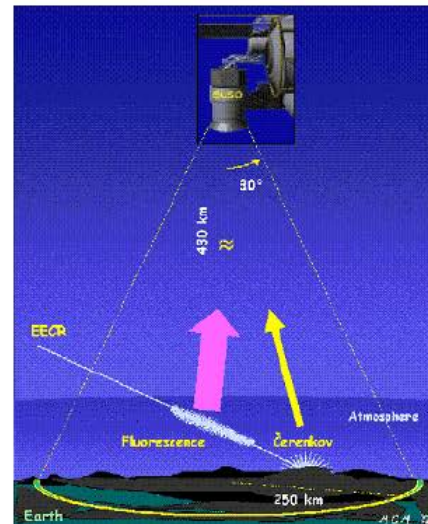

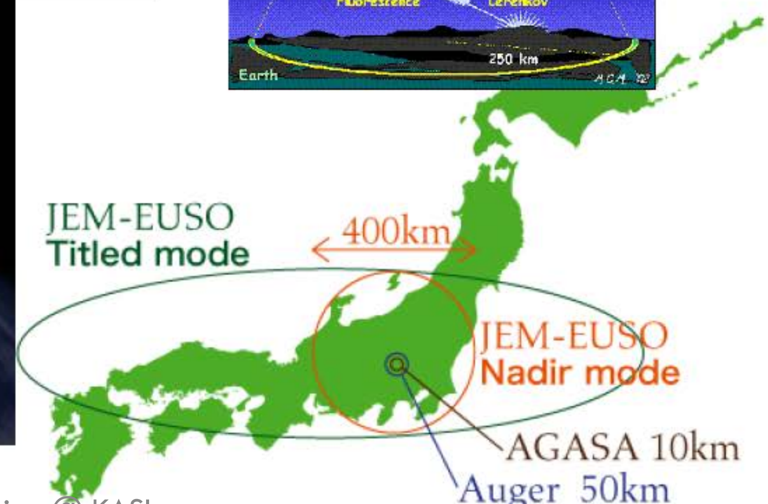

UHECR astronomy

- UHECR flux of the source model

$$F(\hat{r}) \propto \sum_{j \in \mathrm{AGN}} \frac{L}{4\pi d_j^2} \underline{\exp[-(\theta_j(\hat{r}))/\theta_{sj})^2]}$$

the Gaussian smearing angle

- Estimation of the GMF/IGMF strength by the deflection angle
  - Deflection angle by a uniform GMF:

$$\delta_{\mathrm{reg}} \simeq 0.57^\circ Z \left(\frac{D}{1\,\mathrm{kpc}}\right)\left(\frac{10^{20}\,\mathrm{eV}}{E}\right)\left(\frac{B}{10^{-6}\,\mathrm{G}}\right)$$

  - Deflection angle by a turbulent GMF:

$$\delta_{\mathrm{tur}} \simeq 0.15^\circ Z \left(\frac{10^{20}\,\mathrm{eV}}{E}\right)\left(\frac{B_{\mathrm{rms}}}{10^{-6}\,\mathrm{G}}\right)\left(\frac{D}{3\,\mathrm{kpc}}\right)^{1/2}\left(\frac{l_c}{50\,\mathrm{pc}}\right)^{1/2}$$

  - Deflection angle by a IGMF:

$$\delta\theta = 0.8^\circ Z \left(\frac{E}{10^{20}\,\mathrm{eV}}\right)^{-1}\left(\frac{d\,l_c}{10\,\mathrm{Mpc}^2}\right)^{1/2}\left(\frac{B}{10^{-9}\,\mathrm{G}}\right)$$

Summary

- Do we puzzle out the mysteries of UHECR?
- What are their components?

  → proton VS. proton + iron
- Do they get through the GZK?

  → GZK suppression
- Where do UHECRs come from?

  → unclear

References

- Abbasi, R. U., et al. (2008). Astroparticle Physics 30(4): 175.
- Abbasi, R. U., et al. (2010). Physical Review Letters 104(16): 5.
- Abraham, J., et al. (2010). Physical Review Letters 104(9): 7.
- Abreu, P., et al. (2010). Astroparticle Physics 34(5): 314.
- Abu-Zayyad, T., et al. (2012). Astrophysical Journal 757(1): 11.
- Abu-Zayyad, T., et al. (2013). Astrophysical Journal Letters 768(1): 5.
- Bauleo, P. M. and J. R. Martino (2009). Nature 458 (7240): 847.
- Dermer, C. D. and S. Razzaque (2010). Astrophysical Journal 724(2): 1366.
- Harari, D., et al. (2006). Journal of Cosmology and Astroparticle Physics 2006(11): 012.
- Hayashida, N. and K. Honda (2000). arXiv:astro-ph/0008102
- Kim, H. B. and J. Kim (2011.) Journal of Cosmology and Astroparticle Physics(3): 18.
- Kim, H. B. and J. Kim (2013). International Journal of Modern Physics D 22(8): 21.
- Koers, H. B. J. and P. Tinyakov (2009). Journal of Cosmology and Astroparticle Physics(4): 28.
- Ryu, D., et al. (2010). Astrophysical Journal 710(2): 1422.
- Tameda, Y., et al. (2011). Proceedings of the 32nd ICRC, Beijing.